IEEE Access
Multidisciplinary | Rapid Review | Open Access Journal

Date of publication xxxx 00, 0000, date of current version xxxx 00, 0000.

Digital Object Identifier 10.1109/ACCESS.2017.Doi Number

Color Constancy Adjustment using Sub-blocks of the Image

M. A. Hussain and, A. Sheikh-Akbari
School of Computing, Creative Technology and Engineering, Leeds Beckett University, Leeds, UK.

Corresponding author: A. Sheikh-Akbari (e-mail: a.sheikh-akbari@leedsbeckett.ac.uk).

ABSTRACT Extreme presence of the source light in digital images decreases the performance of many image processing algorithms, such as video analytics, object tracking and image segmentation. This paper presents a color constancy adjustment technique, which lessens the impact of large unvarying color areas of the image on the performance of the existing statistical based color correction algorithms. The proposed algorithm splits the input image into several non-overlapping blocks. It uses the Average Absolute Difference (AAD) value of each block's color component as a measure to determine if the block has adequate color information to contribute to the color adjustment of the whole image. It is shown through experiments that by excluding the unvarying color areas of the image, the performances of the existing statistical-based color constancy methods are significantly improved. The experimental results of four benchmark image datasets validate that the proposed framework using Gray World, Max-RGB and Shades of Gray statistics-based methods' images have significantly higher subjective and competitive objective color constancy than those of the existing and the state-of-the-art methods' images.

INDEX TERMS Color Constancy, Color Balance, Gray World.

I. INTRODUCTION

Human vision has the capability to observe and distinguish the color of objects irrespective of the color and intensity of the illuminant under which it is perceived. This capability of the human visual system is known as color constancy [1-2]. The color of objects within a digital image may not seem as they were observed by human vision [3-4]. In conventional imaging devices, the intensity and color of the light source is captured by sensors. Analogous to the human visual system's capability to preserve true color of the scene, imaging devices are equipped with a color correction technique, known as the white balancing function [5-7]. Nevertheless, the existence of an extreme source illuminant could deteriorate the actual color of the objects in the scene captured by a digital camera. The built-in color balancing function of the cameras may not be able to fully mitigate the effect of the extreme illuminant. Even worse, it may bias the image towards the dominant color of the scene. Color constancy algorithms aim to adjust the color of digital images in a way that they appear as if they have been taken from a scene lit by a white illuminant.

In a Lambertian surface, the formation of an image $f = (f_R, \ f_G, \ f_B)^T$ depends on three significant factors including the sensitivity function of the capturing device $(\lambda) = (\rho_R(\lambda), \ \rho_G(\lambda), \ \rho_B(\lambda))^T$, where x and λ denote the spatial coordinate and the wavelength respectively, reflectance property of the surface $S(\boldsymbol{x}, \lambda)$ and the source illuminant colour (λ):

$$f_c(\boldsymbol{x}) = m(x)\int_w I(\lambda)\rho_c(\lambda)S(\boldsymbol{x},\lambda)d\lambda \quad (1)$$

where $m(x)$ refers to the Lambertian shading. In this case, the assumption is that there is a single illuminant and the perceived color of source light e depends on the sensitivity function of the camera $\rho(\lambda)$ and illuminant color $I(\lambda)$:

$$e = \begin{pmatrix} e_R \\ e_G \\ e_B \end{pmatrix} = \int_w I(\lambda)\rho(\lambda)d\lambda \quad (2)$$

In terms of the formation of an image, unknown feature of both $I(\lambda)$ and $\rho(\lambda)$ establish colour constancy as an under-constrained problem, which requires additional assumptions to solve it.

II. RELATED WORK

Over the last two decades, various color constancy adjustment techniques have been proposed by researchers to handle the issue of coloration/color cast within digital images. The existing color constancy techniques, broadly speaking, can be divided into statistics-based, gamut-based, physics-based, learning-based and biologically inspired methods.

For statistics-based methods, the illuminant estimation is not necessary since the images are represented by features that are invariant to the source light. Statistical techniques are based on various assumptions; for example, taking the maximum or the average values of the image three color components to be achromatic [8-9]. Hence, these algorithms use the color information of the image to perform color constancy adjustments. In the following sections, some of the statistic-based methods are discussed. The Gray World method assumes that in a normal, well color balanced image, the average of all the colors is a neutral gray. Hence, the performance of this method depends on the color variation of the image and its color corrected image could be biased to the color of the large uniform regions [8]. The Max-RGB method is a special case of the Retinex theory, which assumes that there is at least one white surface within the image that reflects the chromaticity of the source illuminant. Hence, the chromaticity of the scene light source is estimated as the chromaticity of the maximal red, maximal green and maximal blue color components of the image [9]. Nevertheless, the Max-RGB technique may not always satisfy the requirement of the Retinex theory due to its data dependency. Hence, its color corrected images may be biased toward the dominant color of the scene image. The application of the Max-RGB or White Patch method is further improved by using the sub-sampling process proposed in [10]. In this method, instead of using all the pixels of the image, a random selection of the pixels is used for the color constancy adjustment. The Shades of Gray color correction method assumes that the Minkowski norm-p (associated to the generalized mean or power mean of the image data) of a scene is achromatic [11]. The author of this paper empirically showed that the algorithm produces its best performance when the norm-p equals 6. The next statistic-based method is the Gray Edge proposed in [12], which uses edge information of the objects to perform the color constancy. The Gray Edge hypothesis is based on the assumption that the average absolute derivatives of the image's color components are achromatic. This technique incorporates well-known methods, such as Shades of Gray, Max-RGB or Gray World, and methods based on first- and second-order derivatives to color balance the image. Although applying a low pass filter on the image prior to performing the edge detection increases the strength of the Gray Edge algorithm to noise, it weakens the efficiency of the method. Another statistic-based method called the Weighted Gray Edge was reported in [13]. This technique uses the edge information of different objects in the scene to compute color correction adjustment factors for the whole image.

The gamut mapping method was introduced by Forsyth [14], which assumes that only a small number of colors can be perceived under a source light, known as the canonical gamut. Therefore, color variations within the image (i.e., colors that different to the perceivable colors for a given illuminant) are caused by the deviation in the color of the source light. The gamut mapping algorithm takes an image captured under an unknown illuminant and the pre-determined canonical gamut to adjust the color constancy of the input image. The gamut mapping-based method outperforms the statistics-based methods in many occasions. However, this technique suffers from high computational complexity. Finlayson proposes an extension to the 2D gamut mapping-based method in order to ease its implementation complexity. The author showed that the gamut mapping algorithm can also be calculated in the chromatic space [15]. Finlayson and Hordley in [16] proposed a 3D gamut mapping, which gives slightly higher performance to that of the 2D gamut mapping. An efficient implementation of the gamut mapping method using convex programming was reported in [17], which performs almost similar to that of the original technique. A simpler version of gamut mapping introduced by Mosley and Funt [18] uses a simple cube rather than the convex hull of the pixel values. Gijsenij *et al*. [19] analytically showed that the failure of the diagonal model of the gamut mapping framework can be prevented by adapting the diagonal-offset model [20]. The authors proposed a number of extensions to gamut mapping, which uses some combinations of various n-jet-based gamut mappings and showed that the best estimation of the illuminant is achieved when a feasible intersection of the gamut maps is taken. Gijsenij and Gevers [21] proposed a method to employ the color constancy method that gives the best performance for the input image. The algorithm calculates the Weibull parameters (e.g., grain size and contrast) to extract the image's characteristics. The authors then learn the weighting and the correlation between various image attributes (i.e., textures, edges and SNR) and Weibull parameters by applying a MoG classifier, which results in a selection of the best performing colour constancy method. Their algorithm achieved 20% increase in performance compared to other best performing single-color constancy algorithms.

The methods that exploit the dichromatic reflection model of image formation for color constancy are known as physics-based methods. In such algorithms, the physical interactions between the source illuminant and the object in the scene are considered. This method assumes that all the pixels of one surface are mapped onto a plane in the RGB color space. Therefore, various surfaces are mapped to different planes, and the color of the illuminant can be estimated using the interactions of these planes. Physics-

based techniques encounter difficulties in retrieving specular reflections, and color clipping may also sometimes occur, which affect their performance [22-24]. Finalyson and Schaefer [25] proposed a method that projects the surface pixels by adopting the dichromatic reflection model. This method then employs the Planckian locus of black-body radiators to model the possible illuminants.

Another category of the color constancy techniques is the learning-based algorithms, which use different machine learning algorithms to estimate the scene's illuminants [26-30]. Baron [26] reframed the colour constancy task as a localization problem in log-chromaticity space. It was observed that one could induce a translation in the log-chromaticity histogram by scaling the image's color channels, allowing the implementation of convolutional neural network (CNN) based methods as a solution to the color balancing problem. Bianco *et al.* [27] proposed an illuminant estimation method based on a CNN consisting of one convolutional layer, one fully connected neural network layer and three output nodes. Their algorithm samples the image and neutralizes the contrast of the image using a histogram stretching technique. The method then extracts the activation values of the last hidden layer of each patch and combines them to estimate the illuminant. The authors have obtained convincing performance on a raw image dataset. However, no experimental results have been reported on widely used benchmark image datasets. Another CNN based method was proposed in [28]. This method introduced Minkowski pooling into the context of color constancy to make the network suitable for deep learning. The resulting fully connected layer network produces reliable features for color balancing. Drew *et al.* [29] reported a color constancy approach using a log-relative chromaticity planar called "Zeta Image", which does not need any training data or tunable parameters. Their technique demonstrates superior performance compared to other unsupervised techniques, and the accuracy of light source estimation is similar to the color constancy techniques based on complex procedures requiring tunable parameters and training data. An exemplar method was proposed by Joze and Drew [30], which finds the neighboring surface as an estimation of local source illuminant from the training data using the weak color constant RGB values and the texture features. Xu *et al.* proposed a Global-Based video enhancement algorithm in [31] which meritoriously increases the visual experience of various region of interests within the image or video frames. Their method generates a global tone mapping curve for the whole image by analyzing the features of its different regions of interests. Their results show appropriate and simultaneous improvement on various regions of the processed images. An intra-and-inter-constraint-based (A+ECB) video quality improvement technique was reported by Chen *et al.* [32]. This method identifies the Region of Interests (RoI) within the video frames using the AdaBoost-based object detection algorithm. It then calculates the mean and standard deviation of the resulting RoIs to analyze the features of various RoIs and generates a global piecewise tone mapping curve for the whole frame. They reported that their technique can appropriately and instantaneously improve the visual quality of different RoIs within the image.

Several local estimations and fusion-based color constancy methods were reported in the literature. A significant number of such algorithms assume that a small part of the image is lit by a single illuminant, and based on this hypothesis, these techniques proposed that illuminant must be estimated locally. This is accomplished by the implementation of various segmentation and fusion strategies to handle the influence of multiple illuminants on color constancy adjustment [33-36]. A color constancy method for images of real-world multiple-illuminant scenes was reported in [33]. This technique applies a graph-based algorithm to the image and splits the image into several mini-image regions. This method then calculates a local illuminant estimation for each resulting mini-image region. Their method demonstrated a comparable performance using single-illuminant images to existing state-of-the-art methods. The authors, however, failed to report experimental results on real-word images. Blier *et al.* [34] investigated the application and adaptation of different color constancy algorithms to estimate the scene light sources. Their algorithm segments the input image into superpixels of an approximately similar color. For every superpixel, the algorithm then applies 5 existing statistical methods for illuminant estimation. The results from the applied statistical methods are then fused together to create a single illuminant-color value for each superpixel using a regression-based technique. They reported a median error of 4.1° on non-uniform illumination, which was superior to that of the best-performing estimator on the single-illuminant indoor dataset. Gisenji *et al.* proposed an algorithm to provide color constancy for multi-illuminant scenes' images in [35]. Their algorithm samples the image into P patches using segmentation-based, grid-based, or keypoint-based sampling methods. Each patch is considered to have been illuminated by a single-source illuminant. A pixel-wise illuminant is estimated by grouping together the individually estimated patches and then projecting back onto the original image. Beigpour *et al.* [36] proposed a conditional random field-based color constancy method, which considers both spatial distribution and light source color to estimate the local illuminant. Their algorithm frames the spatial distribution of illuminants as an energy minimization problem and employs a combination of physics-based and statistical-based techniques to estimate multi-illuminant as a single estimation task. The proposed technique demonstrated substantial objective performance on images of scenes lit by multiple light sources.

Another type of multiple-illuminant techniques is built on identifying specific pixels and using them for illuminant estimation. Yang *et al.* [37] uses an illuminant-invariant

measure to efficiently detect the gray pixels of the image, which are used for a scene's illumination estimation. The algorithm is based on the hypothesis that there are some detectable gray pixels within real-world images. Another gray pixel-based color constancy algorithm was reported in [38], which is based on two assumptions. It assumes that the image contains at least a small set of achromatic pixels and that the set of possible light sources is well estimated by black body radiators. Bianco and Schettini [39] showed that the scene light source can be approximated by exploiting the pixels of skin regions of the face using a scale-space histogram filtering.

Elfiky *et al.* [40] studied the relationships between depth, local image statistics and color balancing algorithms. They proposed a technique to determine the color correction algorithm with the best anticipated performance for the image. Their algorithm computes the 3D scene geometry of the image and then exploits the statistics of the image (per layer/depth). These statistics are used to choose the best color balancing technique. Mutimbu and Robles-Kelly [41] proposed a spatially changing light source color estimation method from the scenes illuminated by multiple illuminant. They used a factor graph that is well-defined across the scale space of the input image to estimate a pixelwise illuminant color from a statistically data-driven setting.

Several biologically inspired color constancy models that tries to mimic the functional properties of the human visual system (HVS) using machine learning have been proposed [42-44]. Gao *et al.* [42] proposed an HVS based color correction framework by mimicking the interaction between the single-opponent (SO) cells in the retina and the double-opponent (DO) cells in the primary visual cortex, as well as the possible neurons in the higher visual cortexes. They showed that their framework can generate relatively competitive results in comparison to the state-of-the-art techniques without needing fine-tuning of the algorithm for various dataset separately. Zhang *et al.* [43] reported a framework for computational color adjustment that was motivated by the HVS. The proposed framework emulates the color processing approach found in the retina. Hence, instead of explicitly estimating the scene's illuminant, this model removes the effect of the scene's illuminant. They reported competitive results compared to the state-of-the-art methods for the scenes under different lighting conditions. Akbarnia and Parraga [44] proposed a color constancy model using two overlapping asymmetric Gaussian kernels, where the contrast of the surrounding pixels is used to adjust the kernels' sizes (approximating the change of visual neuron's receptive field size). Finally, the outputs of the most activated visual neuron's receptive fields are used to estimate the light source.

It can be seen that numerous color constancy methods have been proposed to color balance images captured under non-white light sources. These algorithms perform reasonably well when the underlying conditions are satisfied. However, due to the data dependency, their effectiveness is deteriorated when there are some constant color regions in the images, which causes the image being biased towards the color of the dominant unvarying regions.

This paper presents a color correction technique that improves the performance of the existing statistical color constancy methods by excluding the unvarying color areas of the image of being used to compute the color correction factors for the whole image. The proposed method splits the input image into some non-overlapping blocks. Each resulting block's color component is judged to circumvent the uniform color blocks from being contributing to the computation of the color constancy adjustment factors for the image. The existing statistical-based color constancy techniques are then applied to the non-uniform color areas of the image. The experimental results are generated by using three well-known statistical-based methods called Gray World, Max-RGB and Shades of Gray on the images of the four benchmark image datasets. The experimental results demonstrate that the proposed technique subjectively outperforms the statistics-based methods and the state-of-the-art techniques. The results also demonstrate comparable objective results to those of the state-of-the-art methods. The rest of the paper is organized as follows. Section III introduces the proposed technique. The experimental results and evaluation are presented in Section IV. Section V gives the conclusions and future work.

III. COLOR CONSTANCY USING SUB-BLOCKS OF THE IMAGE

A block diagram of the proposed Color Constancy Adjustment using the Sub-blocks of the Image (CCASI) method is shown in Fig. 1(a). The input color image is split into some non-overlapping pixel blocks by the proposed method, labeled B_{11} to B_{nm}, as illustrated in Fig. 1(b). The rest of the proposed technique is as follows [45, 46].

i. The Average Absolute Difference (AAD) value of R, G and B color components is calculated for each resulting block using equation (3):

$$\mathrm{ADD}_C = \frac{\sum_{i=1}^{M}\sum_{j=1}^{N}(|C(i,j)-\bar{C}|)}{N\times M} \qquad (3)$$

where $C \in \{R,\ G,\ B\}$, $\mathrm{AAD_C}$ is the Average Absolute Difference value of the C component, $C(i,j)$ is the value of the C component of the block at position (i,j), $\bar{C}$ is the average value of the C component of the block's pixels and N and M are the size of the block.

ii. The resulting $\mathrm{AAD_R}$, $\mathrm{AAD_G}$ and $\mathrm{AAD_B}$ values are compared with the empirical threshold values for the R, G and B components, which are labeled as T_R, T_G and T_B, respectively. If the $\mathrm{AAD_C}$ of the block color component is greater than its predefined threshold value, this block's component does not represent a uniform color area. Hence, it is selected to contribute to the color constancy adjustment of the whole image.

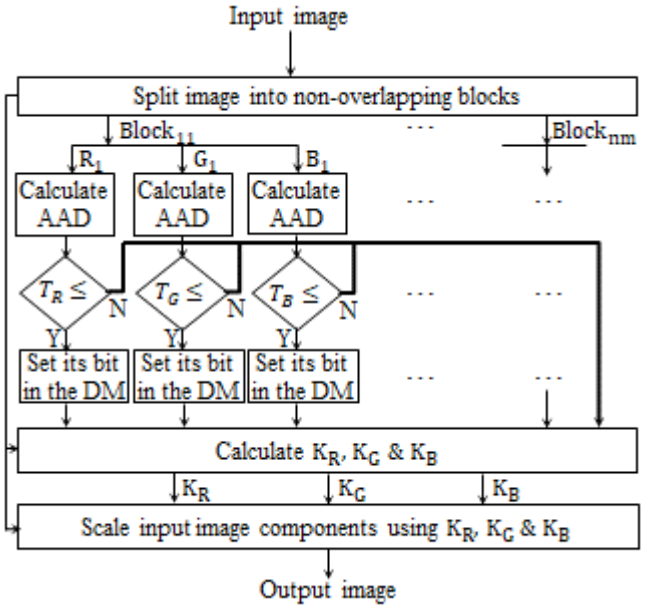

(a)

AAD: Average Absolute Difference
DM: Decision Matrix
T_R, T_G, & T_B: Threshold values for R, G & B components
K_R, K_G K_B: R, G & B components scaling factors

B_{11}	B_{12}	...	...	B_{1m}
B_{21}	B_{22}	...	...	B_{2m}
...	...	B_{ij}	...	...
...	...	...	...	...
B_{n1}	B_{n2}	...	...	B_{nm}

(b)

FIGURE 1. (a) Block diagram of the Color Constancy Adjustment using Sub-blocks of the Image (CCASI) method and (b) non-overlapping blocks of the image.

iii. Set a bit in the Decision Matrix (DM) to represent this block's component (A binary Decision Matrix for each image color component is created and initialized with zeros to keep a record of the selected blocks.).

iv. The scaling factors for the color constancy adjustment are calculated by applying the special instantiations of the more general Minkowski-framework of Finlayson and Trezzi [11] on the selected block of the image, as shown in equation (4):

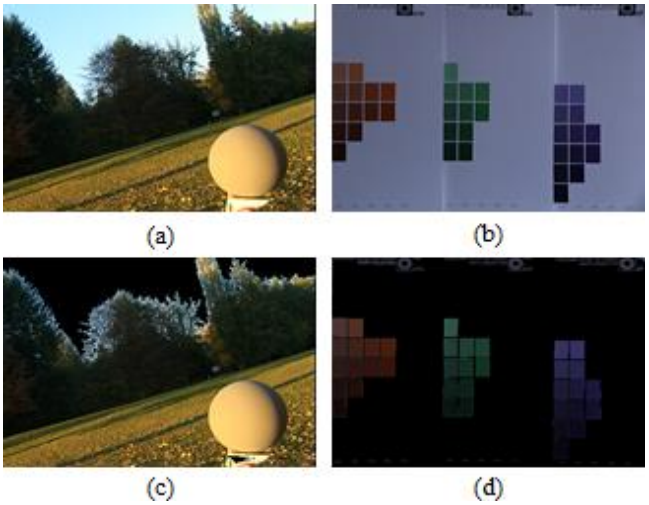

FIGURE 2. (a) original outdoor image, (b) original indoor image, (c) selected areas of the outdoor image and (d) selected areas of the indoor image.

$$K_C = \left(\frac{\int (f_C(x))^p dx}{\int dx}\right)^{1/p} \quad (4)$$

where K_C is the color correction adjustment factor for component C of the image, $C \in \{R, G, B\}$, $f_C(x)$ is the selected pixel value of the component C and p is the Minkowski norm. It was shown in [11] that by setting the value of p to 1, ∞ and 6 in equation 2, it becomes the Gray World, the Max-RGB and the Shades of Gray color constancy methods, respectively.

The resulting scaling factors K_R, K_G and K_B, using the three different techniques, are applied to the input image to adjust its color using the Von Kries diagonal model [47], as shown in equation (5):

$$I_{out} = \begin{pmatrix} K_R & 0 & 0 \\ 0 & K_G & 0 \\ 0 & 0 & K_B \end{pmatrix} \begin{pmatrix} I_R \\ I_G \\ I_B \end{pmatrix} \quad (5)$$

where I_{out} is the color balanced image, K_R, K_G, K_B are the calculated adjustment factors for the color components R, G, B, respectively and I_R, I_G, I_B are the R, G and B color components of the input image, respectively.

To give the reader a visual sense of the selected blocks, the input images and their selected blocks for one outdoor and one indoor image are shown in Fig. 2, where black areas represent discarded blocks. From Fig. 2, it can be seen that the uniform areas of the input images are identified and excluded from contributing to the color constancy adjustment.

IV. EXPERIMENTAL RESULTS

The performance of the proposed Color Constancy Adjustment using the Sub-blocks of the Image (CCASI)

method is assessed and compared with the statistics-based techniques and the state-of-the-art methods using four image datasets. These benchmark datasets include both multiple- and single-illuminant images. Both subjective and objective analysis was used to assess the performance of the proposed technique and compared with state-of-the-art methods.

Sub-section 4.1 introduces the benchmark datasets. The evaluation criteria are explained in Sub-section 4.2. Sub-section 4.3 justifies the selection of the empirical parameters. Finally, the experimental results and their discussions are presented in sub-section 4.4.

4.1. DATASETS

SFU Laboratory dataset [48]: The SFU Laboratory dataset is divided into two group of images, both of which contain colorful objects captured under laboratory settings. The first group, Group A, includes 32 scenes with multiple objects. Group B includes 20 scenes of a single object.

The Gray Ball dataset [49]: The Gray Ball dataset is comprised of 11,340 images, with each image having a resolution of 240×360. The images vary significantly in terms of lighting conditions and contain both single- and mixed-illuminants. Each image contains a gray ball. Because this dataset was captured using a video camera, many of the images are nearly identical in nature. For this work, two hundred images were selected by merit of having significant variation to generate subjective results.

Gehler's Color Checker dataset [50]: This dataset consists of 568 images taken both indoors and outdoors. The images contain various objects, people, and places, but all include a Macbeth color checker somewhere in the scene. From this dataset, one hundred images of various scenes under both single- and multiple-illuminant conditions were selected to generate subjective results.

The MIMO dataset [36]: The MIMO dataset consists of twenty real-world and fifty-eight laboratory images. All images in this dataset are taken under multi-illuminant conditions.

4.2. EVALUATION METHODS

The image color constancy quality measurement criteria are categorized into two groups: objective and subjective. For objective analysis, the performance of a color balancing method is assessed by computing the distance between the ground truth and color balanced image. Both the Euclidean and angular distance are measured, of which the latter is the most frequently used method in the literature. The angular error measures the angular distance between the color corrected image and its ground truth image using equation (6):

$$angular\ error = \cos^{-1}(\hat{I}_G . \hat{I}_{CC}) \quad (6)$$

where $\hat{I}_G$ and $\hat{I}_{CC}$ indicate the normalized ground truth and the normalized color balanced image vectors, respectively.

The angular error enables one to compare the performances of two different algorithms since it represents the accuracy of the under-investigation method's performance. To assess and compare the performance of the color constancy algorithms over a large set of images using a single statistic such as the angular error, the mean or the median of the angular error over a set of images is calculated. The algorithm with the lowest mean or median angular error is considered the best-performing algorithm. There are some debates on the use of a single summary statistic for comparing various techniques. As a result, this single statistic may not always sufficiently summarize the underlying distribution or carry adequate information to draw the conclusion that the one with the lowest mean has the highest performance [51]. In [39, 42, 52, 53]; the authors used the Wilcoxson Sign Test [54] to determine the statistical significance of the resulting angular errors on a large number of images. The experimental results show that the application of the mean or median angular error is not always inconsistent with the achieved objective qualities. Furthermore, Finlayson and Zakizadeh [55] have identified a problem with this metric. The authors have observed that the same scene, when viewed under two different colored lights for the same algorithm, leads to different recovery errors.

Considering the inconsistency of objective quality assessment methods, such as the angular error, and the fact that the human eyes are the final evaluator in assessing the color constancy of the images, in this paper, both subjective and objective assessment methods are used to compare the visual quality of the color-corrected images.

4.3. PARAMETER SELECTION

The performance of the color variability assessment of the proposed Color Constancy Adjustment using the Sub-blocks of the Image (CCASI) technique as a function of its thresholds values, T_R, T_G and T_B, was assessed using images from the four previously mentioned image datasets [45]. The empirical threshold values for each block's color component are determined as follows:

i. Apply the block selection algorithm on the blocks of the image component.

ii. Visually review the selected blocks.

iii. If the blocks comprising unvarying color regions are identified and discarded, go to step v.

iv. Add 0.05 to the current threshold value of the color and go to step ii.

v. Allocate the current threshold value to the empirical threshold value.

The average of the resulting threshold values for a collection of images from the four image datasets were selected as the general empirical values for the proposed technique, which are $T_R = 2$, $T_G = 1.5$ and $T_B = 1$. The empirical thresholds' values presented above can also be determined by using an objective method to define initial

empirical thresholds' values and then using a subjective evaluation to increase their accuracies. This could significantly reduce the time and efforts needed to determine precise empirical values for thresholds.

To elaborate on the threshold selection in terms of the Average Absolute Difference (AAD) values of the color components, one sample image from the Gray Ball dataset with 600 sub-blocks of size 12 ×12 is presented in Fig. 3. In this figure, three blocks containing different color variabilities are selected (highlighted with a red color border). For each block, the AADs are calculated and tabulated in Table 1. From Table 1, one can observe that the AADs of block 1, which represent an unvarying color region, are below the empirically determined threshold values.

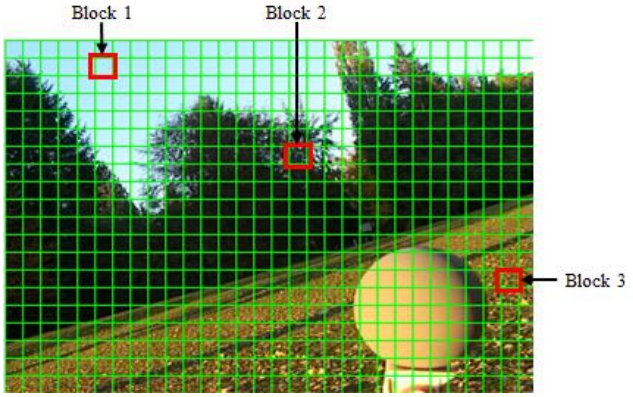

FIGURE 3. Sub-blocks of a sample image from the Gray Ball image dataset.

4.4. EXPERIMENTAL RESULTS

In this section, both the subjective and objective results for the proposed color constancy method using the Gray World, Max-RGB and Shades of Gray statistical-based methods on the images of the four previously mentioned benchmark datasets are presented and compared with those of the statistical and the state-of-the-art techniques.

4.4.1 SUBJECTIVE RESULTS

To elaborate on the achieved subjective visual qualities using the proposed color constancy method and to enable the reader to compare the visual qualities of the proposed technique's images with the images of other statistical and state-of-the-art techniques' images, six sample images from SFU, MIMO, Color Checker and the Gray Ball datasets, which cover a variety of sceneries and include natural- and laboratory-setting objects (illuminated by either a single or multiple illuminants), are shown in Figs. 4-9.

Fig. 4 shows a sample image from the SFU laboratory image dataset that exhibits blue color cast and the ground truth of the image as well as its color balanced images using the 2nd Order Gray Edge, Weighted Gray Edge, Double Opponency, Proposed Color Constancy Adjustment using Sub-blocks of the Image with Gray World (CCASI-GW), Max-RGB (CCASI-Max-RGB) and Shades of Gray (CCASI-SG) methods' images. From Fig. 4, it can be seen that the 2nd Order Gray Edge image (Fig. 4c) is overcorrected since it exhibits higher intensity compared to the ground truth. The Weighted Gray Edge image (Fig. 4d) appears to be slightly darker than the ground truth image. The Double Opponency's image (Fig. 4e) shows improved color correction in comparison to the 2nd Order Gray Edge and Weighted Gray Edge images. Nevertheless, it exhibits higher brightness compared to the ground truth image. The proposed CCASI-GW method's image (Fig. 4f) has a slightly lower intensity of a white background compared to that of the ground truth image. However, the colors of the blocks within the image are very similar to those of the ground truth image. The Proposed CCASI-Max-RGB method's image (Fig. 4g) has an almost identical visual quality to that of the ground truth. However, its median angular error is greater than that of the proposed CCASI-GW technique's image. The proposed CCASI-SG method's image (Fig. 4h) has a small bluish color cast, but it has kept the intrinsic intensity of the original image. Overall, the proposed CCASI-Max-RGB technique's image exhibits the maximum color correction among all the presented methods' images.

TABLE I
AVERAGE ABSOLUTE DIFFERENCE (AAD) VALUES OF THE THREE SELECTED BLOCKS.

Sub-block / AAD	Block 1	Block 2	Block 3
R_{AAD}	1.54	23.9	20.8
G_{ADD}	1.40	16.6	17.1
B_{ADD}	0.86	12.1	17.8

Fig. 5 shows a sample image from the MIMO (Lab) dataset and the ground truth of the image as well as its color balanced images using the 2nd Order Gray Edge, Weighted Gray Edge, Double Opponency, Proposed Color Constancy Adjustment using Sub-blocks of the Image with Gray World (CCASI-GW), Max-RGB (CCASI-Max-RGB) and Shades of Gray (CCASI-SG) methods' images. From Fig. 5, it can be seen that the 2nd Order Gray Edge method's image (Fig. 5c) still has some yellowish color cast, particularly on the mug. The Weighted Gray Edge's image (Fig. 5d) exhibits a higher contrast with respect to the ground truth image and has some yellow color cast. The Double Opponency method's image (Fig. 5e) exhibits higher color constancy than the 2nd Order Gray Edge and Weighted Gray Edge images. However, the image still has some color casts. The proposed CCASI-GW, CCASI-Max-RGB, and CCASI-SG methods' images (Fig. 5f-h) illustrate the uppermost color correction amongst all the other techniques' images. However, the CCASI-GW image (Fig. 5f) is the closest in appearance to the ground truth image.

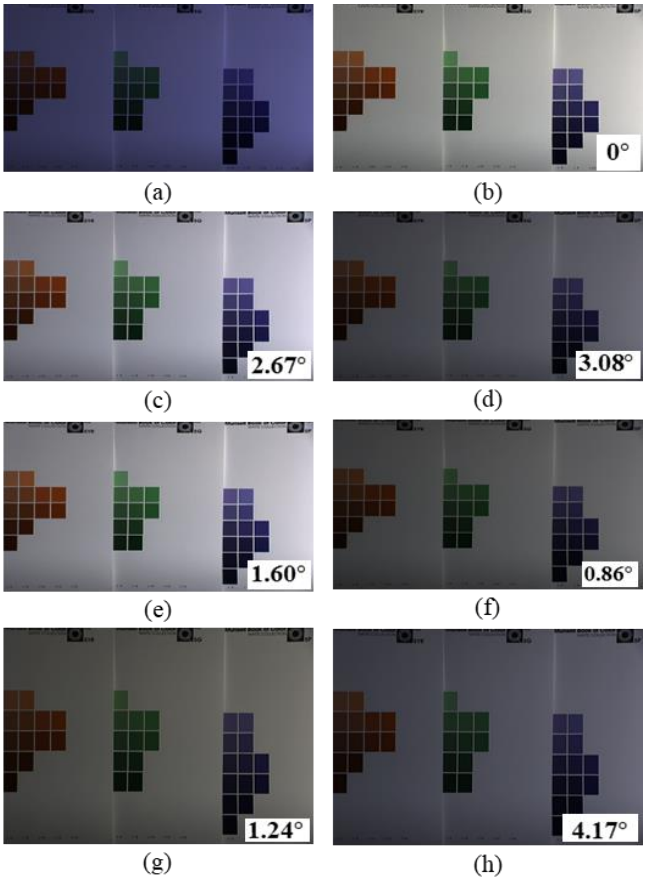

FIGURE 4. Original, ground truth and color balanced images of an image from the SFU (laboratory) dataset: a) Original image, b) Ground truth, c) 2nd Order Gray Edge, d) Weighted Gray Edge, e) Double Opponency, f) Proposed CCASI-GW, g) CCASI-Max-RGB and h) CCASI-SG methods' images.

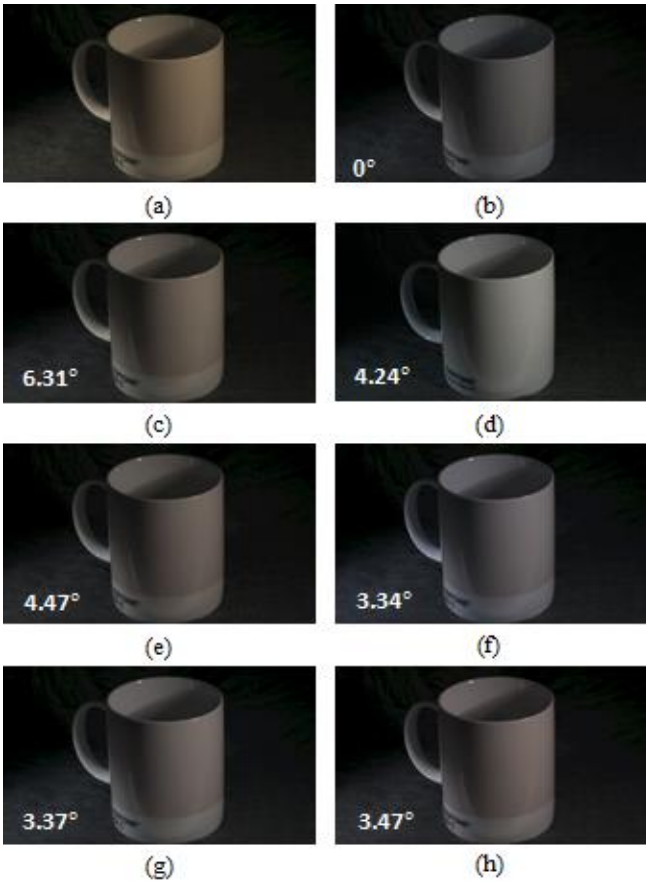

Figure 5. Original, ground truth and color balanced images of an image from the MIMO (Lab) dataset: a) Original image, b) Ground truth, c) 2nd Order Gray Edge, d) Weighted Gray Edge, e) Double Opponency, f) Proposed CCASI-GW, g) CCASI-Max-RGB and h) CCASI-SG methods' images.

Fig. 6 illustrates a sample image from Gehler's Color Checker dataset, which represents a scene with colorful objects and a color checker chart, as well as the ground truth of the image and its color balanced images using the 2nd Order Gray Edge, Weighted Gray Edge, Double Opponency, Proposed Color Constancy Adjustment using Sub-blocks of the Image with Gray World (CCASI-GW), Max-RGB (CCASI-Max-RGB) and Shades of Gray (CCASI-SG) methods' images. The original image contains a heavy green color cast. From Fig. 6, it is clear that the 2nd Order Gray Edge method's image (Fig. 6c) exhibits a slightly reddish tone. The Weighted Gray Edge method's image (Fig. 6d) appears to have reduced green color cast. The Double Opponency method's image (Fig. 6e) exhibits much higher color constancy than those of the Gray Edge-2 and Weighted Gray Edge methods' images. However, its color cast is still evident. The proposed CCASI-GW, CCASI-Max-RGB, and CCASI-SG methods' images, as shown in Figs. 6f-h, demonstrate the highest color constancy. The CCASI-GW's image is visually the closest image to the ground truth despite its median angular error being higher than that of CCASI-Max-RGB's image.

Fig. 7 illustrates a sample image from the Gray Ball dataset with a yellow color cast and its color balance images using Exemplar, Color Cat, the proposed Color Constancy Adjustment using Sub-blocks of the Image with Gray World (CCASI-GW), Max-RGB (CCASI-Max-RGB) and Shades of Gray (CCASI-SG) methods' images. From Fig. 7, it can be seen that Exemplar and Color Cat methods' images exhibit some levels of yellow color casts (shown in Figs. 7b and 7c). The proposed CCASI-GW method's image (Fig. 7d) appears to be a shot under canonical light as the presence of the source illuminant is significantly reduced. However, the median angular error to the ground truth obtained using the gray sphere of the ball area is the uppermost among all the techniques. The proposed CCASI-Max-RGB and CCASI-SG techniques' images (shown in Figs. 7e and 7f) contain an infinitesimal amount of color cast, despite low median angular errors. In summary, the proposed CCASI-GW method's image has the uppermost subjective color correction among all the other techniques' images.

Fig. 8a illustrates a sample image from Gehler's Color Checker dataset. This image was captured under a bright yellow illuminant and includes an area of cloudy sky and a large green grass surface with a color checker chart on the grass. It can be observed from the image that the white, narrow paths next to the buildings are well-lit. Fig. 8b show

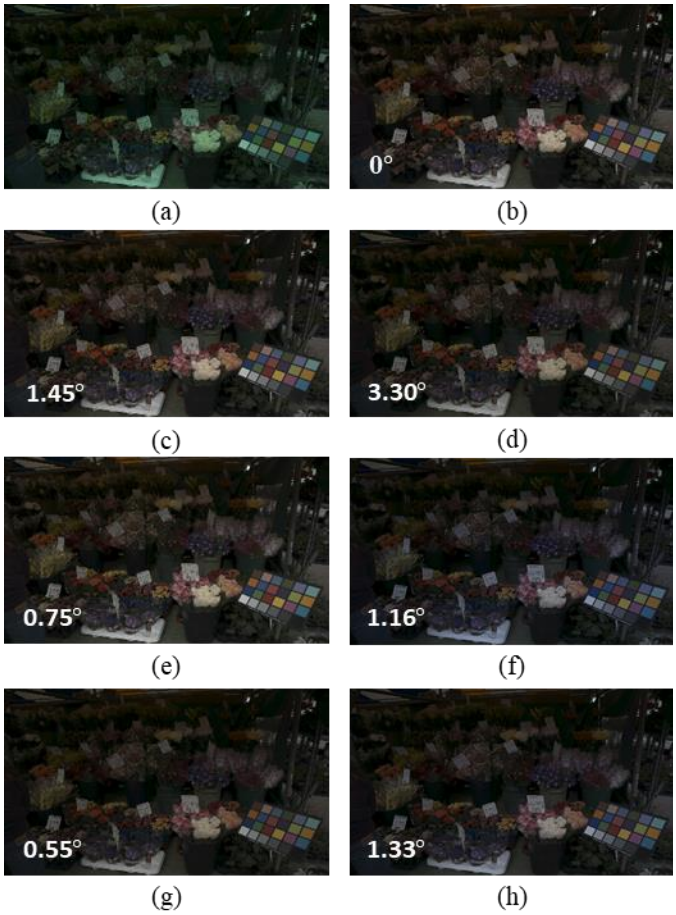

FIGURE 6. Original, ground truth and color balanced images of an image from the Gehler's Color Checker dataset: a) Original image, b) Ground truth, c) 2nd Order Gray Edge, d) Weighted Gray Edge, e) Double Opponency, f) Proposed CCASI-GW, g) CCASI-Max-RGB and h) CCASI-SG methods' images.

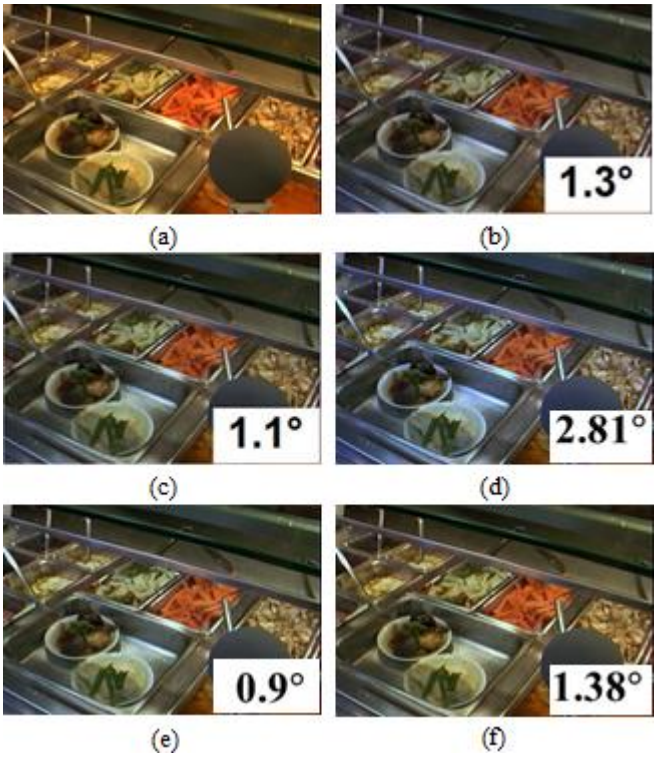

FIGURE 7. Original and color balanced images of an image from the Gray Ball dataset: Original image, b) Ground truth, b) Exemplar, c) Color Cat, f) Proposed CCASI-GW, g) CCASI-Max-RGB and h) CCASI-SG methods' images.

the perfectly color balanced ground truth image. The Max-RGB technique's image is shown in Fig. 8c. From this image, one can observe that the green ground area of the image exhibits a clear color improvement, but a very subtle light-yellow color on the white path areas of the image is evident. The Shades of Gray technique's image is presented in Fig. 8d. From this image, it is observed that the green grass area of the image has higher color constancy in comparison to the input image, while it still has a minor yellow color cast on the white paths of the image. The 1st Order Gray Edge technique's image is shown in Fig. 8e. This image exhibits lower color constancy performance in comparison to the images of Figs. 8c-d due to the increased illuminant on the image scene. Fig. 8f illustrates the 2nd Order Gray Edge technique's image. This image is nearly identical to that of the 1st Order Gray image presented in Fig. 8e. Fig. 8g illustrates the Weighted Gray Edge technique's image. Areas within this image, specifically, the buildings and the nearby path, demonstrate greater yellow color casting compared to that of its input image. The proposed CCASI-GW technique's image presented in Fig. 8h shows a significant removal of the color cast. However, the image is slightly overcorrected compared to the ground truth image. Fig. 8i is the suggested CCASI-Max-RGB method's image. This image exhibits a significant reduction in the oversaturation and seems to be captured under white light. Fig. 8j is the proposed CCASI-SG method's image. This image demonstrates a distinct natural color on the image objects. In particular, the small white square of the color chart and the white path seem to be very similar to that of the ground truth image at a 400% zoom view on a 42-inch LED monitor. Moreover, the lowest angular error obtained by the proposed method shows superior performance against other compared techniques [46].

From Fig. 9, it is clear that the original image has a strong yellow color cast. The 2nd Order Gray Edge technique's image (Fig. 9c) has an extreme bluish color cast. The Weighted Gray Edge technique's image (Fig. 9d) has a slightly lower color cast. The Sub- sample method's image (Fig. 9e) presents an improved color correction. However, there is an infinitesimal influence of the source illuminant on the upper right corner of the white shelf. The proposed CCASI-GW, CCASI-Max-RGB, and CCASI-SG method's images (shown in Figs. 9f-9h) show the highest color constancy. Among the proposed techniques' images, the CCASI-SG (shown in Figs. 9f-9h) show the highest color constancy. Among the proposed techniques' images, the CCASI-SG technique's image illustrates the uppermost color correction. The objects in this image have very similar color to their respective objects in the ground truth image.

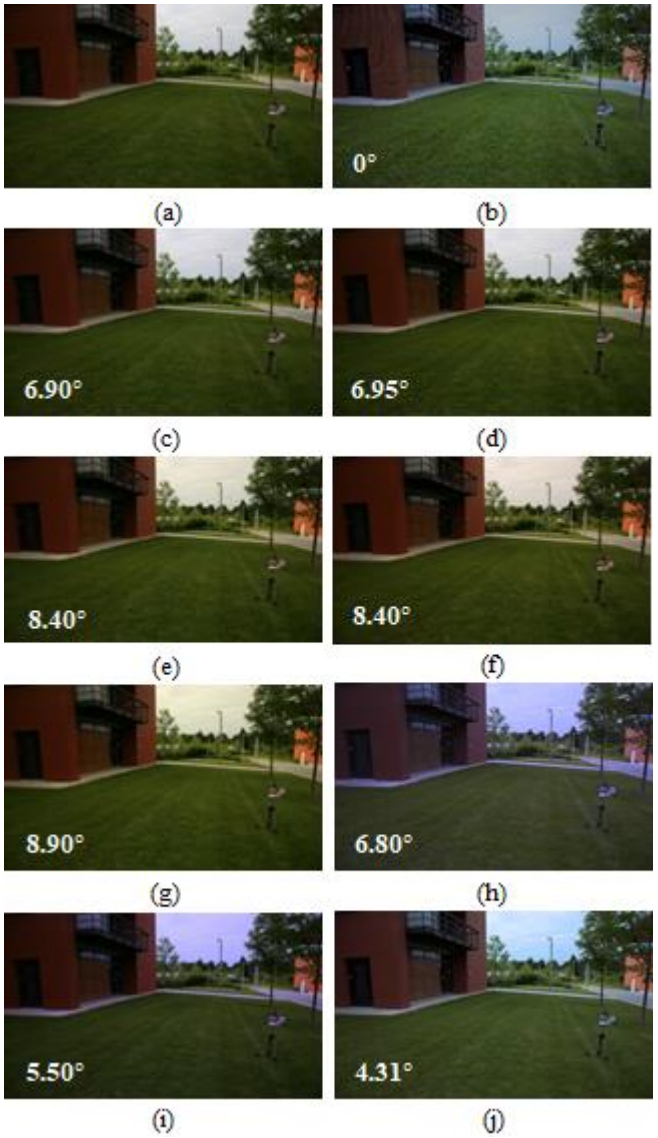

FIGURE 8. Original and color balanced images from various techniques: a) Original image from Gehler's Color Checker dataset, b) Ground truth, c) Max-RGB, d) Shades of Gray, e)1st Order Gray Edge, f) 2nd Order Gray Edge, g) Weighted gray edge, h) Proposed CCASI-GW, i) Proposed CCASI-Max-RGB, and j) Proposed CCASI-SG methods' images.

To generate the Mean Opinion Score (MOS), the proposed algorithm and the state-of-the-art methods have been applied to the randomly selected 200 images and 100 images from the Gray Ball dataset and the Gehler's dataset, respectively, and all the images of the MIMO dataset and the SFU dataset. Ten independent observers were shown the aforementioned images to generate subjective results. Each image was scored from 1 to 5, with 1 being the lowest color constancy and 5 being the uppermost color correction. The resulting scores for each color constancy technique were averaged and are reported in Table 2. From Table 2, one can observe that the proposed technique's images exhibit the uppermost MOS in comparison to the other methods' images and the proposed CCASI-GW technique's MOS is higher than those of the two other proposed methods' MOSs.

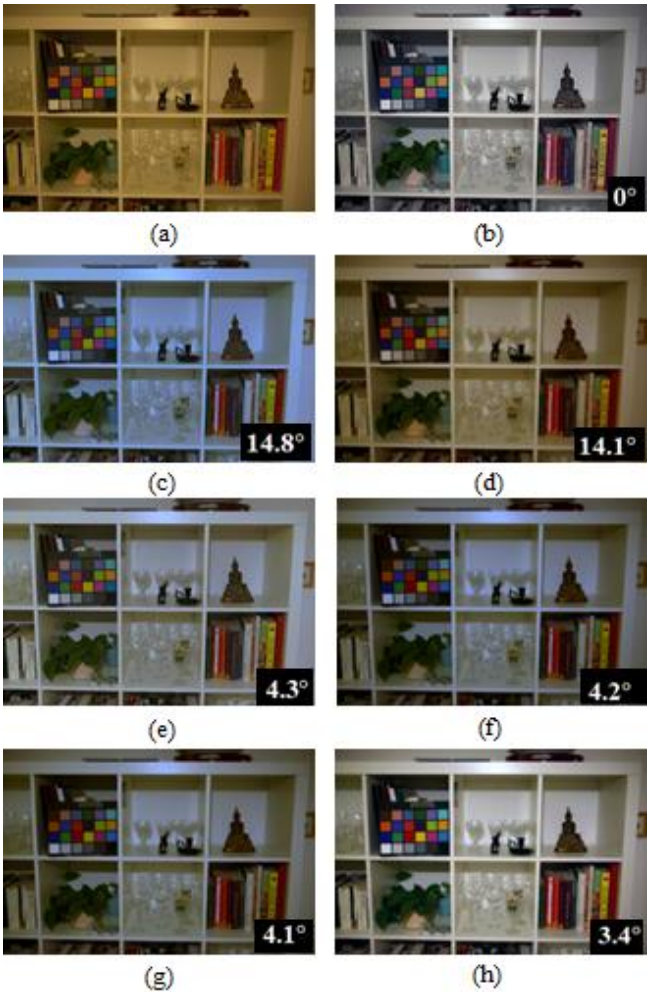

FIGURE 9. Original, ground truth and color balanced images of an image from the Gehler's Color Checker dataset: a) Original image, b) Ground truth, c) 2nd Order Gray Edge, d) Weighted Gray Edge, e) Sub-sample, f) proposed CCASI-GW, g) CCASI-Max-RGB and h) CCASI-SG methods' images.

4.4.2 OBJECTIVE ASSESSMENT

To assess the objective performance of the proposed Color Constancy Adjustment using the Sub-blocks of the Image with Gray World (CCASI-GW), Max-RGB (CCASI-Max-RGB) and Shades of Gray (CCASI-SG) techniques with the Gray World, Max-RGB and Shades of Gray, 1st and 2nd Order Gray Edge, Pixel-based Gamut Mapping [14], Edge-based Gamut Mapping [19], Exemplar method [30], Gray Pixel [37] and Adaptive Surround Modulation (ASM) [44] color constancy methods, they were applied to the images of the Gray Ball dataset. The average mean and median angular errors of the resulting images were calculated and can be found in Table 3. Table 3 demonstrates that the proposed techniques generally outperform all the statistics-based methods. The proposed CCASI-GW, CCASI-Max-RGB and CCASI-SG images have average mean angular errors of 4.5°, 5.7° and 4.5°, respectively, which are well below the mean angular error of all the statistical methods. Moreover, the average median angular errors of the proposed CCASI-Max-

TABLE II
MEAN OPINION SCORE (MOS) OF THE PROPOSED AND THE STATE-OF-THE ART TECHNIQUES

	Methods							
Dataset	WGE	Gisenji *et al.*	MIRF	Gray Pixel	Exemplars	Proposed CCASI-GW	Proposed CCASI-Max-RGB	Proposed CCASI-SG
MIMO	3.71	3.80	4.18	3.97	4.03	4.20	4.11	3.98
Gray Ball	4.0	3.25	3.88	3.84	3.67	4.07	4.02	3.89
Gehler's Color Checker	3.80	3.76	3.91	4.03	3.79	4.16	4.11	3.96
SFU	3.91	4.02	3.97	4.07	4.07	4.15	4.19	4.02

RGB and CCASI-SG are 4.2° and 4.6°, respectively, which are lower than those of all the statistical methods. However, the average median angular error of the first proposed CCASI-GW method is 4.8°, which is less than that of all the statistical methods except the 1st-Order Gray Edge method. The average median angular error of this method is 4.7°, which is very close to that of the first proposed CCASI-GW method, which is 4.8°. These objective results imply that the proposed methods' images have the highest objective qualities among the statistical-based methods' images. From Table 3, it can be seen that the three proposed methods deliver lower mean and median angular errors compared to those of the gamut-based methods. However, with respect to the learning-based methods, the proposed techniques produce very competitive objective results.

To demonstrate the objective performance of the proposed Color Constancy Adjustment using the Sub-blocks of the Image with Gray World (CCASI-GW), Max- RGB (CCASI-Max-RGB) and Shades of Gray (CCASI-SG) techniques with that of the Gray World, Max-RGB and Shades of Gray, 1st- and 2nd-Order Gray Edge, Pixel-based Gamut Mapping, Edge-based Gamut Mapping and Natural Image Statistics [21] color constancy approaches were applied to the images of the Gelhar's Color Checker dataset. The average mean and median angular errors of the resulting images were calculated and can be found in Table 4. From Table 4, one can see that the lowest mean and median angular errors are obtained by the proposed CCASI-Max-RGB technique's images among the images of both the statistical- and gamut-based methods. This implies that the CCASI-Max-RGB method's images have the uppermost objective color correction amongst the images of both the statistical- and gamut-based methods. Moreover, the average mean and median angular errors of the other two proposed CCASI-GW and CCASI-SG techniques are comparable to the high-performing statistical- and gamut-based methods.

To objectively compare the performance of the proposed Color Constancy Adjustment using the Sub-blocks of the Image with Gray World (CCASI-GW), Max-RGB (CCASI-Max-RGB) and Shades of Gray (CCASI-SG) techniques with Gisenji *et al.* [35] and MIRF [36] color constancy

TABLE III
AVERAGE MEAN AND MEDIAN ANGULAR ERRORS OF THE PROPOSED AND OTHER COLOR CONSTANCY METHODS' IMAGES ON THE GRAY BALL DATASET

Method	**Mean**	**Median**
Statistics-based methods		
Gray World	7.9°	7.0°
Max-RGB	6.8°	5.3°
Shades of Gray	6.1°	5.3°
1st Order Gray Edge	5.9°	4.7°
2nd Order Gray Edge	6.1°	4.9°
CCASI-GW	4.5°	4.8°
CCASI-Max-RGB	5.7°	4.2°
CCASI-SG	4.5°	4.6°
Gamut-based methods		
Pixel-based Gamut	7.1°	5.8°
Edge-based Gamut	6.8°	5.8°
Learning-based methods		
Exemplar-based	4.4°	3.4°
Gray Pixel (std)	4.6°	6.2°
ASM	4.7°	3.8°

TABLE IV
AVERAGE MEAN AND MEDIAN ANGULAR ERRORS OF THE PROPOSED AND OTHER COLOR CONSTANCY METHODS' IMAGES ON THE GEHLER'S COLOR CHECKER DATASET

Method	**Mean**	**Median**
Statistics-based methods		
Gray World	9.8°	7.4°
Max-RGB	8.1°	6.0°
Shades of Gray	7.0°	5.3°
1st Order Gray Edge	5.2°	5.5°
2nd Order Gray Edge	7.0°	5.0°
Weighted Gray Edge	6.6°	4.7°
CCASI-GW	5.6°	5.8°
CCASI-Max-RGB	4.9°	4.5°
CCASI-SG	6.8°	6.5°
Gamut-based methods		
Pixel-based Gamut	6.9°	4.9°
Edge-based Gamut	7.7°	5.0°
Natural Image Statistics	6.1°	4.5°

TABLE V
COMPARATIVE PERFORMANCES ON THE MIMO (REAL) IMAGE DATASET

	Gisenji *et al.*		**MIRF**		**Proposed method**	
	Mean	Median	Mean	Median	Mean	Median
Gray World	4.4°	4.3°	3.7°	3.4°	4.12°	3.96°
Max-RGB	4.2°	3.8°	4.1°	3.3°	3.8°	3.5°
Shades of Gray	-	-	-	-	5.0°	4.9°

TABLE VI
COMPARATIVE PERFORMANCES ON THE MIMO (LABORATORY) IMAGE DATASET

	Gisenji *et al.*		**MIRF**		**Proposed method**	
	Mean	Median	Mean	Median	Mean	Median
Gray World	6.4°	5.9°	3.1°	2.8°	4.36°	3.93°
Max-RGB	5.1°	4.2°	3.0°	2.8°	4.96°	4.12°
Shades of Gray	-	-	-	-	4.60°	4.20°

approaches, they were applied to the images of the MIMO dataset. The average mean and median angular errors of the resulting real and the laboratory images were calculated and are tabulated in Table 5 and Table 6, respectively. The experimental results for the Gisenji *et al.* and MIRF methods using Gray World and Max-RGB were taken from [36]. It must be mentioned that the Gisenji *et al.* and MIRF techniques do not use the Shades of Gray method. From Tables 5 and 6, it is evident that the proposed CCASI- GW and CCASI-Max-RGB methods' images have lower average mean and median angular errors compared to Gisenji *et al.*'s images, where their images' angular errors are very close to those of the MIRF method's images.

V. CONCLUSIONS AND FUTURE WORK

This paper presented a color constancy method that improved the performance of the existing techniques by excluding the uniform color areas of the image from contributing to the color constancy of the image. Hence, this technique splits the input image into some non-overlapping blocks. The average absolute difference value of each block is computed and used to determine if the block has sufficient color information to contribute to the color constancy adjustment of the image. The experimental results were generated by applying the three statistical-based color constancy methods of the Gray World, Max-RGB and Shades of Gray techniques on the images from four benchmark image datasets. The quality of the resulting images is both subjectively and objectively assessed and compared to those of other statistical and state of the art techniques. The results show the merit of the proposed technique.

Integration of more low-level images features, e.g. image saliency, for color constancy has potential to improve the subjective visual quality of the images. This has been less reported in the literature, which is a future direction for this research.

REFERENCES

[1] K. Yanlin Qian, J.K. Chen, J. Kämäräinen, J. Nikkanen and J. Matas, "Deep structured-output regression learning for computational color constancy," *International Conference on Pattern Recognition*, Cancun, 2016, pp. 1899-1904.

[2] J. Simão, H. J. A. Schneebeli and R. F. Vassallo, "An Iterative Approach for Color Constancy," *Joint Conference on Robotics: SBR-LARS Robotics Symposium and Robocontrol*, Sao Carlos, 2014, pp. 130-135.

[3] A. Gijsenij, T. Gevers, and J. Van de Weijer, "Computational Color Constancy: Survey and Experiments," *in Image Processing, IEEE Transactions on* , vol.20, no.9, pp.2475-2489, September 2011.

[4] B. R. Ciprian, "Multi-frame Auto White Balance," Signal Processing Letters, IEEE , vol.18, no.3, pp.165,168, March 2011.

[5] S. Bianco, C. Cusano and R. Schettini, "Single and Multiple Illuminant Estimation Using Convolutional Neural Networks," *in IEEE Transactions on Image Processing*, vol. 26, no. 9, pp. 4347-4362, Sept. 2017.

[6] N. Banić, and S. Lončarić, "Color Cat: Remembering Colors for Illumination Estimation," *in IEEE Signal Processing Letters*, vol. 22, no. 6, pp. 651-655, June 2015.

[7] F. J. Chang and S. C. Pei, "Color constancy via chromaticity neutralization: From single to multiple illuminants," *2013 IEEE International Symposium on Circuits and Systems (ISCAS2013)*, Beijing, 2013, pp. 2808-2811.

[8] G. Buchsbaum, "A spatial processor model for object colour perception," *Journal of the Franklin Institute*, vol. 310, no. 1, pp. 1–26, July 1980.

[9] E. Land, "The retinex theory of colour vision," *Scientific American*, vol. 237, no. 6, pp. 108–128, December 1977.

[10] N. Banić and S. Lončarić, "Improving the white patch method by subsampling," *2014 IEEE International Conference on Image Processing (ICIP)*, Paris, 2014, pp. 605-609.

[11] G.D. Finlayson, and E. Trezzi, "Shades of grey and colour constancy," *Proc. IS&T/SID Color Imaging Conf*., pp. 37-41, 2004.

[12] J. van de Weijer, T. Gevers, and A. Gijsenij, "Edge based colour constancy," *IEEE Trans on Image Processing*, pp.2 207-2217, 2007.

[13] A. Gijsenij, T. Gevers, and J. Van de Weijer, "Improving Color Constancy by Photometric Edge Weighting," *IEEE Trans. on Pattern Analysis and Machine Intelligence*, vol. 34(5):918-929, 2012.

[14] D. Forsyth, "A novel algorithm for color constancy," *International Journal of Computer Vision*, vol. 5, no. 1, pp. 5–36, 1990.

[15] G. Finalyson, "Color in perspective," *IEEE Transactions on Pattern Analysis and Machine Intelligence*, vol. 18, no. 10, pp. 1034–1038, 1996.

[16] G. Finlayson and S. Hordley, "Improving gamut mapping color constancy," *IEEE Transactions on Image Processing*, vol. 9, no. 10, pp. 1774–1783, 2000.

[17] G. Finlayson and R. Xu, "Convex programming color constancy," in *IEEE Workshop on Color and Photometric Methods in Computer Vision*, in conjunction with ICCV'03, 2003, pp. 1–8.

[18] M. Mosny and B. Funt, “Cubical gamut mapping colour constancy,” in *IS&T’s European Conference on Color in Graphics, Imaging and Vision*, Joensu, 2010, pp.466-470.

[19] A. Gijsenij, T. Gevers, and J. Van De Weijer. Generalized gamut mapping using image derivative structures for color constancy. *International Journal of Computer Vision*, vol.86, no. 23:127–139, 2010.

[20] G. Finlayson, S. Hordley, and R. Xu, “Convex programming colour constancy with a diagonal-offset model,” in *IEEE International Conference on Image Processing*, Norwich, 2005, pp. 948–951.

[21] A. Gijsenij and T. Gevers, "Color Constancy Using Natural Image Statistics and Scene Semantics," in *IEEE Transactions on Pattern Analysis and Machine Intelligence*, vol. 33, no. 4, pp. 687-698, April 2011.

[22] S. Tominaga and B. Wandell, “Standard surface-reflectance model and illuminant estimation,” *Journal of the Optical Society of America*, vol. 6, no. 4, pp. 576–584, 1989.

[23] G. Healey, “Estimating spectral reflectance using highlights,” *Image and Vision Computing*, vol. 9, no. 5, pp. 333–337, 1991.

[24] R. Tan, K. Nishino, and K. Ikeuchi, “Color constancy through inverse-intensity chromaticity space,” *Journal of the Optical Society of America*, vol. 21, no. 3, pp. 321–334, 2004.

[25] G. Finlayson and G. Schaefer, “Solving for colour constancy using a constrained dichromatic reflection model,” *International Journal of Computer Vision*, vol. 42, no. 3, pp. 127–144, 2001.

[26] J. T. Barron, "Convolutional Color Constancy," *IEEE International Conference on Computer Vision (ICCV)*, Santiago, 2015, pp. 379-387.

[27] S. Bianco, C. Cusano and R. Schettini, "Color constancy using CNNs," *IEEE Conference on Computer Vision and Pattern Recognition Workshops* (CVPRW), Boston, MA, 2015, pp. 81-89.

[28] D. Fourure, R. Emonet, E. Fromont, D. Muselet, A. Trémeau, and C. Wolf, "Mixed pooling neural networks for color constancy," *IEEE International Conference on Image Processing*, Phoenix, AZ, pp. 3997-4001, 2016.

[29] M. Drew, H. Vaezi Joze, and G. Finlayson, “Specularity, the zeta image, and information-theoretic illuminant estimation,” *in Proc. ECCV*, Florence, Italy, 2012.

[30] H. R. V. Joze and M. S. Drew, "Exemplar-Based Color Constancy and Multiple Illumination," in *IEEE Transactions on Pattern Analysis and Machine Intelligence*, vol. 36, no. 5, pp. 860-873, May 2014.

[31] N. Xu, W. Lin, Y. Zhou, Y. Chen, Z. Chen and H. Li, "A new global-based video enhancement algorithm by fusing features of multiple region-of-interests," 2011 Visual Communications and Image Processing (VCIP), Tainan, 2011, pp. 1-4.

[32] Y. Chen, W. Lin, C. Zhang, Z. Chen, N. Xu and J. Xie, "Intra-and-Inter-Constraint-Based Video Enhancement Based on Piecewise Tone Mapping," in IEEE Transactions on Circuits and Systems for Video Technology, vol. 23, no. 1, pp. 74-82, Jan. 2013.

[33] C. Riess, E. Eibenberger and E. Angelopoulou, "Illuminant color estimation for real-world mixed-illuminant scenes," *IEEE International Conference on Computer Vision Workshops (ICCV Workshops)*, Barcelona, 2011, pp. 782-789.

[34] M. Bleier *et al.*, "Color constancy and non-uniform illumination: Can existing algorithms work?", *IEEE International Conference on Computer Vision Workshops*, pp. 774-781, 2011.

[35] A. Gijsenij, R. Lu and T. Gevers, "Color Constancy for Multiple Light Sources," in *IEEE Transactions on Image Processing*, vol. 21, no. 2, pp. 697-707, Feb.2012.

[36] S. Beigpour, C. Riess, J. van de Weijer, and E. Angelopoulou, "Multi-Illuminant Estimation with Conditional Random Fields," in *IEEE Transactions on Image Processing*, vol. 23, no. 1, pp. 83-96, Jan. 2014.

[37] K. F. Yang, S. B. Gao and Y. J. Li, "Efficient illuminant estimation for color constancy using grey pixels," *IEEE Conference on Computer Vision and Pattern Recognition (CVPR)*, Boston, MA, 2015, pp. 2254-2263.

[38] B. Mazin, J. Delon and Y. Gousseau, "Estimation of Illuminants From Projections on the Planckian Locus," *in IEEE Transactions on Image Processing*, vol. 24, no. 6, pp. 1944-1955, June 2015.

[39] S. Bianco and R. Schettini, "Adaptive Color Constancy Using Faces," in *IEEE Transactions on Pattern Analysis and Machine Intelligence*, vol. 36, no. 8, pp. 1505-1518, Aug. 2014.

[40] N. Elfiky, T. Gevers, A. Gijsenij and J. Gonzàlez, "Color Constancy Using 3D Scene Geometry Derived From a Single Image," in *IEEE Transactions on Image Processing*, vol. 23, no. 9, pp. 3855-3868, Sept. 2014.

[41] L. Mutimbu and A. Robles-Kelly, "Multiple Illuminant Color Estimation via Statistical Inference on Factor Graphs," in *IEEE Transactions on Image Processing*, vol. 25, no. 11, pp. 5383-5396, Nov. 2016.

[42] S. B. Gao, K. F. Yang, C. Y. Li and Y. J. Li, "Color Constancy Using Double-Opponency," in *IEEE Transactions on Pattern Analysis and Machine Intelligence*, vol. 37, no. 10, pp. 1973-1985, Oct. 1 2015.

[43] X. S. Zhang, S. B. Gao, R. X. Li, X. Y. Du, C. Y. Li and Y. J. Li, "A Retinal Mechanism Inspired Color Constancy Model," in *IEEE Transactions on Image Processing*, vol. 25, no. 3, pp. 1219-1232, March 2016.

[44] A. Akbarinia and C. A. Parraga, "Colour Constancy Beyond the Classical Receptive Field," in *IEEE Transactions on Pattern Analysis and Machine Intelligence*, vol.40, no. 8, pp. 1-14.

[45] M. A. Hussain, A. S. Akbari and B. Mallik, "Colour constancy using sub-blocks of the image," 2016 International Conference on Signals and Electronic Systems (ICSES), Krakow, 2016, pp. 113-117.

[46] M. A. Hussain and A. S. Akbari, "Max-RGB Based Colour Constancy Using the Sub-blocks of the Image," *2016 9th International Conference on Developments in eSystems Engineering (DeSE)*, Liverpool, 2016, pp. 289-294

[47] J. von Kries, “Influence of adaptation on the effects produced by luminous stimuli,” in *Sources of Color Vision, D. MacAdam, Ed. MIT Press*, 1970, pp. 109–119.

[48] K. Barnard, L. Martin, A. Coath, and B. Funt. A comparison of computational color constancy algorithms – part ii: Experiments with image data. Image Processing, *IEEE Transactions on*, 11(9):985 – 996, sep 2002.

[49] Ciurea, F., Funt, B., “A Large Image Database for Color Constancy Research”, *Proceedings of the Imaging Science and Technology Eleventh Color Imaging Conference*, November 2003, Scottsdale, USA, pp. 160-164.

[50] P. Gehler, C. Rother, A. Blake, T. Sharp, and T. Minka, "Bayesian colour constancy revisited," *IEEE Conference on Computer Vision and Pattern Recognition (CVPR)*, pp. 1-8, June 2008.

[51] S. D. Hordley and G. D. Finlayson, "Re-evaluating colour constancy algorithms," *Proceedings of the 17th International Conference on Pattern Recognition*, 2004. ICPR 2004., 2004, pp. 76-79 Vol.1.

[52] L. Shi, W. Xiong, and B. Funt, “Illumination estimation via thin-plate spline interpolation”, *Journal of the Optical Society of America*, Vol. 28, Issue 5, pp. 940-948, 2011.

[53] A. Gijsenij, T. Gevers, and M.P. Lucassen, “Perceptual Analysis of Distance Measures for Color Constancy Algorithms,” *J. Optical Soc. of Am. A*, vol. 26, no. 10, pp. 2243-2256, 2009.

[54] F. Wilcoxon, “Individual Comparisons by Ranking Methods”, *Biometrics Bulletin*, Vol. 1, No. 6, pp. 80-83, 1945.

[55] G. D. Finlayson, R. Zakizadeh and A. Gijsenij, "The Reproduction Angular Error for Evaluating the Performance of Illuminant Estimation Algorithms," *in IEEE Transactions on Pattern Analysis and Machine Intelligence*, vol. 39, no. 7, pp. 1482-1488, July 1, 2017.

MD AKMOL HUSSAIN is pursuing his PhD at Leeds Beckett University, UK. He received a B.Eng. degree in Electronics and Communication from University of Wolverhampton in 2011 and a Post-Graduate Certificate (Mainly by Research) from the University of Gloucestershire in 2014. His research interests include computer vision, image processing and image forensics.

DR. AKBAR SHEIKH AKBARI is a Senior Lecturer in School of Computing, Creative Technologies & Engineering at Leeds Beckett University. He has a BSc (Hons), MSc (distinction) and PhD in Electronic and Electrical Engineering. After completing his PhD at Strathclyde University, he joined Bristol University to work on an EPSRC project in stereo/multi-view video processing. He continued his career in industry, working on real-time embedded video analytics systems. His main research interests include signal processing, hyperspectral image processing, source camera identification, image/video forgery, image hashing, biometric identification techniques, assisted living technologies, compressive sensing, camera tracking using retro-reflective materials, standard and non-standard image/video codecs, e.g., H.264 and HEVC, multi-view image/video processing, color constancy techniques, resolution enhancement methods, edge detection in low-SNR environments and medical image processing.